V European Conference on Computational Fluid Dynamics
ECCOMAS CFD 2010
J. C. F. Pereira and A. Sequeira (Eds)
Lisbon, Portugal, 14–17 June 2010

IMPROVING THE RESISTANCE OF A SERIES 60 VESSEL WITH A CFD CODE

J. M. A. Fonfach[*], C. Guedes Soares[†]

[*]Centre for Marine Technology and Engineering (CENTEC)
Technical University of Lisbon, Instituto Superior Técnico
Av. Rovisco Pais, 1049-001 Lisboa, Portugal
e-mail: jose.fonfach@mar.ist.utl.pt, guedess@mar.ist.utl.pt

Key words: Computational Fluid Dynamics, Ship Hydrodynamics, Free Surface Flow, Turbulent Models, Hull Shape Optimization

Abstract. *An hydrodynamic study was carried out of a series 60 vessel model using a CFD RANS (Reynolds Averaged Navier-Stokes Equations) based code, with the aim of calculating the pressure gradient and shear stresses of the flow around the vessel, and the associated wave train generated at the interface of two fluids (free Surface), for Froude numbers in the range of 0.18 to 0.34. The data were validated with previous published experimental tests. Different mesh size was used in the present study to determine the most appropriate one. The use of a zone with turbulent properties is a fundamental aspect in viscous flow simulation. For the solution of the governing equations two turbulence models for the turbulent viscosity are evaluated. They are: Shear Stress Transport (SST) and the K-ε model. Subsequent to obtaining these results, a study to optimize the hydrodynamic resistance was conducted, so that the hull of the ship was modified by adding a bow bulb, which were analyzed with two different lengths, obtaining the best alternative*

1 INTRODUCTION

The design and optimization of the hull lines have traditionally been performed on the basis of scaled models tested in towing tanks. This method is today the most reliable in the prediction of hydrodynamic properties of the ship. Analytical methods are not used due to the complexity of the governing equations of real flows complicated by the existence of free surface, viscous phenomena and the complex ship geometry.

In these days with the development of new numeric tools, the advances in computer technology and the increase capability of data processing, Computational Fluid Dynamic (CFD) has made remarkable progress and allowed good results to be obtained. The interest and demand of the industry to implement new methods is one of the most important reasons that influence the development of CFD.

Ships have been built with bulbous bows as part of the hull, but the hydrodynamic design of bulbous bows is still difficult, because of expensive tank tests necessary in the design of the bows, even at the preliminary design stage. It is vital to define the hydrodynamic performance of the hull, to calculate the engine power, capable to overcome the hydrodynamic resistance produced by the interaction of the hull with the flow. Thus it is important to design the hull forms such that they can operate economically [1-2]. It is necessary to understand the complicated flow characteristics for an optimal hull design, which includes a low drag and high propulsive efficiency. For better knowledge of the flow around the hull, it is important to have reliable and accurate data, about the physical phenomena in the interaction flow-ship. The data of the experimental tests which describe the local flow details are invaluable for the validation of the CFD models.

There have been some experimental data of the flow around the ship models available for validation of CFD. The international towing tank conference (ITTC) summarized available benchmark data base for CFD Validation for resistance and propulsion of a ship, for the cargo-container ship, series 60 and turbulent measurement test case are given in [3-4]. Previously two workshops were presented for the computational analysis flow around ships, HSVA/Dyne tanker and a series 60 model were chosen for the test case [5].

However the progress that has been achieved in the experimental tests has not decreased the interest of knowing in detail the flow field, with better information of the near-wall flow, associated with the motion of hull. This information is not offered by the experimental method; on the other hand CFD have a good performance in giving characteristics of the behavior of the flow that often improve development of the hull form. The cost and time required for the computation are lower than for tank tests. The CFD has been integrated in to researching and the industry, for example it is being used in design of ships for the prediction of viscous flow with free surface around the hull, the flow separation to design appendices and propeller-hull interaction.

Viscous flow computation for ships began in the 60´s, with the simplified boundary layer equation being solved. In this approach, the boundary layer can be calculated acceptably in the hull, however, this formulation failed in the predicting flow at stern. In the 80´s a large number of RANS (Reynolds Averaged Navier-Stokes) methods were developed for ship stern flow. The stern flow prediction capabilities were improved rather remarkably around 1990. However, CFD simulations near the propeller were less satisfactory, due to shape of the boundary layer in the propeller zone. Later, it was realized, that the reason for the inability to predict was the inadequate modeling of turbulence. This lead to the implementation of more advanced models, such as the k-ω turbulence model and the Reynolds stress model [6].

The modern viscous flow codes, which solve the RANSE, have the ability to simulate efficiently the turbulent flow problems around ships. The two models most used in CFD to solve the turbulent phenomena, are the standard k-ε model and the Shear Stress transport (SST) k-ω, the performance of which models was studied in [7] dealing with the prediction of the reattachment length of flow. The k-ω model gave very good comparison to experimental data while the k-ε model predicted a significantly shorter length. However, the k-ω model overpredicted the spreading rates around the free shear layer due to inaccurate prediction of eddy viscosity value.

Free surface problems such as the wave making problem were simulated with viscous flow codes depending on whether the computational grid adapts to the shape or the position of the free surface. Therefore, two major approaches widely applied to the free surface computations are the so-called interface-tracking method, e.g. a moving mesh and the interface-capturing method, e.g. the volume of fluid method (VOF) proposed by Hirt and Nichols [8] to deal with free surface boundary problems.

The aim of this study is the use of CFD code for a ship design. For that effect, the performance of the series 60 ship model was improved as a result of changes in the hull form. First a study of the naked hull was performed, which analyzed the mesh sensitivity and validated numerical data. Then two different bulbs were designed to reduce the resistance of the hull. The models were calculated with the commercial software CFX version 12.1.

2 MATHEMATICAL MODEL

In CFX, the Reynolds-averaged Navier–Stokes (RANS) equations for the momentum transport and continuity equation for mass conservation are equations governing the motion of a three-dimensional steady, incompressible and viscous turbulent flow. The homogenous multiphase Eulerian–Eulerian fluid approach utilizes Volume of Fluid method (VOF) to describe the free surface flow problem mathematically.

The utilized VOF method is a fixed grid technique designed for two or more fluids, where in each cell of a mesh it is necessary to use only one value for each dependent variable defining the fluid state, which can be defined by a function α_q (where q represent the fraction of volume; q = 1, 2,..).The value of this variable is unity at any point occupied by fluid and zero in the other case. The average value of α in a cell represents the position of the interface of the fluid. In particular, a unit value of α would correspond to a cell full of fluid, while a zero value would indicate that the cell is empty, so the cells with α values between zero and one must, the contain a free surface. The tracking of the interface is accomplished by solving the continuity equation of the volume fraction. For the *q* liquid, this equation is written as follow:

$$\frac{\partial \alpha_q}{\partial t} + u_i \frac{\partial \alpha_q}{\partial x_j} = 0 \tag{1}$$

where the constraints are given by:

$$\sum_{q=1}^{n} \alpha_q = 1 \tag{2}$$

and for incompressible flows, the first term of the continuity equation is:

$$\frac{\partial \alpha_q}{\partial t} = 0 \tag{3}$$

The density of the whole fluid in each cell is evaluated by the volume-fraction-average of all liquids in the cell:

$$\rho = \sum \alpha_q \rho_q \tag{4}$$

All other properties (e.g., viscosity ν) are computed in the same way. The momentum equation is dependent on the volume fractions of all liquids through the properties ρ and ν. The Navier-Stokes equation can be written in Cartesian tensor form as follows:

$$\frac{\partial u_i}{\partial t} + u_j \frac{\partial ui}{\partial_j} = -\frac{1}{\rho}\frac{\partial p}{\partial x_i} + \frac{\partial}{\partial x_i}\left(\nu \frac{\partial u_i}{\partial x_j}\right) \tag{5}$$

where for steady flow, the velocity-time can be written as:

$$\frac{\partial u_i}{\partial t} = 0 \tag{6}$$

where u is the velocity in the stream direction, ρ is the fluid density, ν is the kinematic viscosity of the flow and p is the pressure.

The Navier-Stokes equation cannot be resolved properly for the effects of high frequency turbulence, because the computational resources do not allow the current generation of sufficiently fine mesh to properly resolve the small-scale vortice length. For this reason, the efforts in Computational Fluid Dynamics are directed to the solution of the Reynolds equations. These equations are obtained using the definition of average time.

The flow is separated into mean $(\overline{U})$ and fluctuating (u') components in the RANS approach to turbulence:

$$U = \overline{U} + u' \tag{7}$$

the time averaging velocity component is defined as:

$$\overline{U} = \frac{1}{T}\int_0^T U dt \tag{8}$$

where T is the averaging time of the simulation, usually chosen to be large compared to the typical timescale of turbulent fluctuations. Substituting into the Navier-Stokes equations in steady flow for time averaging, one obtains the time averaged Navier-Stokes equations:

$$\overline{u_j}\frac{\partial \overline{u_i}}{\partial_j} = -\frac{1}{\rho}\frac{\partial \overline{p}}{\partial x_i} + \frac{\partial}{\partial x_i}\left(\nu \frac{\partial \overline{u_i}}{\partial x_j} - \overline{u_i u_j}\right) \tag{9}$$

where, the statistical averaging of the Navier-Stokes equations give rises to the unknown term, is defined in eq.(10):

$$\overline{-u_i u_j} = \nu_t\left(\frac{\partial u_i}{\partial x_j} + \frac{\partial u_j}{\partial x_i}\right) - \frac{2}{3}k\delta_{ij} \tag{10}$$

which are the correlation between the fluctuating velocity components and is known as the Reynolds Stress term. The existence of the Reynolds stress means there is no longer

a closed set of equations, and turbulence model assumptions are needed to estimate the unknowns to solve this closure problem

Two models were used to calculate the turbulent viscosity. In CFD, the standard k-ε and Shear Stress Transport k-ω are the two most widely used models in this category. The standard k-ε turbulence model solves the flow based on the assumption that the rate of production and dissipation of turbulent flows are in near-balance in energy transfer. The dissipation rate, ε of the energy is written as:

$$\varepsilon = \frac{k^{3/2}}{L} \tag{11}$$

where k is the kinetic energy of the flow and L is the length scale involved. This is then related to the turbulent viscosity ν_t based on the Prandtl mixing length model:

$$\nu_t = \rho C_\mu \frac{k^2}{\varepsilon} \tag{12}$$

where C_μ is an empirical constant and ρ is the density the flow, applying this to the equations governing fluid flow, the k equation of the standard k-ε model is written as:

$$U_i \frac{\partial(\rho U_j k)}{\partial x_j} = \frac{\partial}{\partial x_j}\left(\frac{\nu_t}{\sigma_\varepsilon}\frac{\partial k}{\partial x_j}\right) + \nu_t \frac{\partial U_i}{\partial x_j}\left(\frac{\partial U_i}{\partial x_j} + \frac{\partial U_j}{\partial x_j}\right)\frac{\partial U_i}{\partial x_j} - \rho\varepsilon \tag{13}$$

and the ε equation:

$$U_i \frac{\partial(\rho U_j \varepsilon)}{\partial x_j} = \frac{\partial}{\partial x_j}\left(\frac{\nu_t}{\sigma_\varepsilon}\frac{\partial \varepsilon}{\partial x_j}\right) + C_{\varepsilon 1}\frac{\varepsilon}{k}\nu_t \frac{\partial U_i}{\partial x_j}\left(\frac{\partial U_i}{\partial x_j} + \frac{\partial U_j}{\partial x_j}\right) - \rho C_{\varepsilon 2}\frac{\varepsilon^2}{k} \tag{14}$$

based on extensive examination of a wide range of turbulent flows, the constant parameters used in the equations take the following values,

$$C_\mu = 0.09;\ C_{\varepsilon 1} = 1.44;\ C_{\varepsilon 2} = 1.92;\ \sigma_k = 1.0;\ \sigma_\varepsilon = 1.3$$

Shear Stress Transport k-ω two equations model was developed as an alternative to cover the deficiencies of the standard k-ε model at the walls. The Shear Stress Transport k-ω is similar in structure to the k-ε model but the variable ε is replaced by the dissipation rate per unit kinetic energy. The k equations in the Shear Stress Transport model are written as:

$$U_i \frac{\partial(\rho U_j k)}{\partial x_j} = \frac{\partial}{\partial x_j}\left(\frac{\nu_t}{\sigma_\varepsilon}\frac{\partial k}{\partial x_j}\right) + \nu_t \frac{\partial U_i}{\partial x_j}\left(\frac{\partial U_i}{\partial x_j} + \frac{\partial U_j}{\partial x_j}\right)\frac{\partial U_i}{\partial x_j} - \rho k\omega \tag{15}$$

and the ω equation:

$$U_i \frac{\partial(\rho U_j \varepsilon)}{\partial x_j} = \frac{\partial}{\partial x_j}\left(\frac{\nu_t}{\sigma_\varepsilon}\frac{\partial \omega}{\partial x_j}\right) + \alpha\frac{\omega}{k}\nu_t \frac{\partial U_i}{\partial x_j}\left(\frac{\partial U_i}{\partial x_j} + \frac{\partial U_j}{\partial x_j}\right) - \beta\rho\omega^2 \tag{16}$$

where:

$$\nu_t = \rho\frac{k}{\omega} \tag{17}$$

Although the two equation models (k-ω and k-ε) provide a good compromise between complexity and accuracy among RANS models, the applications are restricted

to steady type of flow. Thus, solution is sought to achieve both computational efficiency and the capability of predicting the chaotic nature of flow such as vortex shedding.

3 SHIP MODEL

The ship model used for this study is a series 60 with block coefficient (C_B) of 0.6, which is a single-propeller merchant type ship and is a standard for ship-hydrodynamics research, and was chosen because, is one of used by ITTC research program. The characteristic of naked hull model used for the experimental and computational test are, given bellow, and the longitudinal profile of the 3D model is shown in Figure 1.

Length between perpendicular	(Lbp)	7.000	[m]
Breadth	(B)	0.933	[m]
Draft	(T)	0.373	[m]
Displacement	(∇)	1.462	[m^3]
Wetted Surface Area	(S)	8.349	[m^2]

Figure 1: longitudinal profile of the 3D model.

4 EXPERIMENTAL SETUP

To compare and validate the numerical results, use have been made of the experimental results presented by the ITTC Cooperative Experiment on a Series 60 Model, at the Ship Research Institute in the study “Flow Measurement and Resistance Test” [4].

In the experiments, the resistance test was carried out under free condition. The range of Froude number (*Fn*) was 0.07 to 0.34 and its step is 0.01. The resistance force was measured by a resistance dynamometer of the strain gauge type which has the capacity of 20kg and a tolerance of 0.05% of the full scale.

The wave profiles along the hull surface were measured by photographs at values of *Fn* = 0.18; 0.22; 0.25; 0.28; 0.30; 0.32 and 0.34. The horizontal and vertical scales were drawn on the model surface for this purpose. The photographs were taken by the three 35mm cameras.

The viscous flow field was measured using 5-hole Pitot tube, which is the NPL type (apex angle is 100 deg.) and its diameter is 5mm. The ship model was fixed to the towing carriage in order to assure the accuracy of measuring position. The Froude number was set to 0.18, for calibration.

The water conditions in the towing tank are shown in Table 1:

T°	21.50	°C
ρ	101.75	kgs^2/m^4
ν	$0.963\ 10^{-6}$	m^2/s

Table 1: The environment condition measured in the Towing tank.

5 COMPUTATIONAL DOMAIN AND GRID GENERATION

The geometry of the hull and the volume of control of the grid were obtained in appropriate external software, and the molded offsets of the transverse section of the model were obtained from the polynomial definition of the cross section for series 60.

The modeled surface of hull was compared with the experimental model; the difference was only 0.2%, and thus it was considered that the surface was modeled optimally by the generated mesh. The volume of control was chosen to be of box shape. The height of the computational domain is $1.25L_{bp}$ and its width is taken to be of $1.5L_{bp}$ due to the symmetry of the problem. The domain inlet boundary is at a distance of 1.5L ahead of the ship, while the outlet boundary is located at $2.6L_{bp}$ from the ship stern.

The grid generator ICEM CFD was used for meshing the computational domain with unstructured tetrahedral grid and different mesh sizes were considered for the analysis of resistance in naked hull condition. The mesh size for the hull and free surface are summarized in Table 2 and are shown in Figures 3 and 4. Mesh sensitivity studies were performed to explore the effect of different topology and local refinement to observer accuracy on the result, In ICEM CFD the option Low transition was chosen to refine the mesh gradually in the zone of interest until a remote zone of the domain. Unstructured tetrahedral grid was chosen because it is easily adjustable to complex geometry; however this type of mesh increases the computational cost.

Mesh N°	Hull Size	F.S. Size	Domain N° Node
Mesh N°1	2%L	2%L	425,940
Mesh N°2	0.5%L	2%L	596,313
Mesh N°3	0.5%L	1%L	1,874,160
Mesh N°4	0.25%L	1%L	2,391,549

Table 2: Different size mesh used in the hull and Free Surface (F.S.). L is the Length between perpendiculars.

In the free surface and hull surface a prismatic layer mesh was applied (see Figure 2), with an exponential increment between layers. The initial height and the number of layers are presented in the Table 3. The parameter selected was that the total layer height in the interface zone is twice the draft of the hull, and the total thickness around to hull approximately equal to one quarter of draft. The prismatic layer mesh has been used in the all cases except for mesh N°1.

Item	N° Layers	Initial height
Hull	20	0.035
F. S.	20	0.001

Table 3: Parameters for Prism layer mesh applied in the hull and Free Surface.

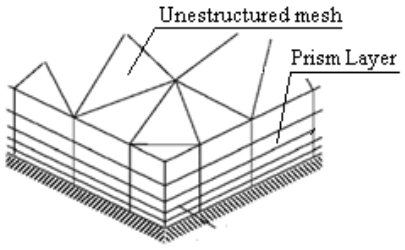

Figure 2: Scheme of grid used in the computational domain.

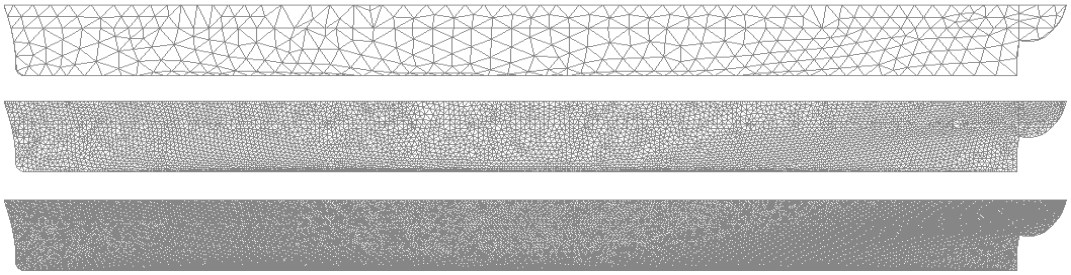

Figure 3: Computational Grid on Series 60 surface, at different size mesh.

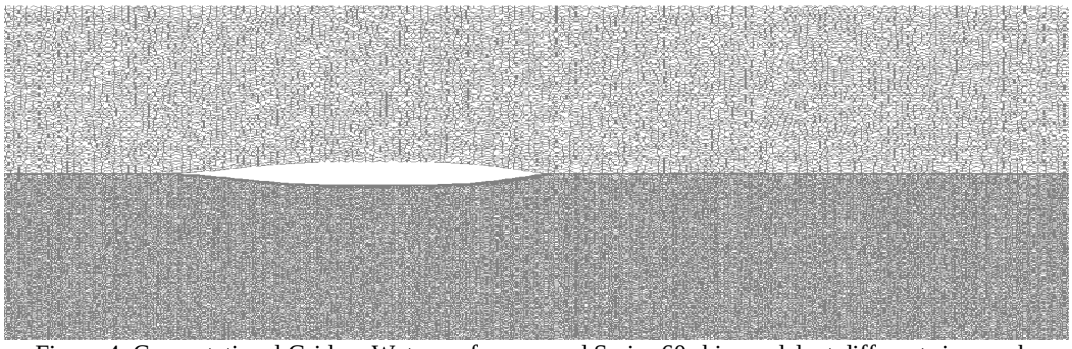

Figure 4: Computational Grid on Water surface around Series 60 ship model, at different size mesh.

6 BOUNDARY CONDITIONS AND SIMULATION CRITERIA

For free surface calculations, the air and water flow around the series 60 ship model was simulated using the standard homogenous Volume of Fluid (VOF) model (or free surface model) available in CFX 12.1. In the VOF model, a single moment equations is shared by the fluid volume fraction of each of the fluids in each computational cell is tracked throughout the domain, surface tension was not applied in the models. The coupled volume fraction solution algorithm was used to improve the convergence. The sink and trim of the hull was not taken into account, thus it was considered that the hull was fixed and the computations were run steady in time.

The standard k-ε and shear stress transport k-ω turbulent model was employed in the CFD simulations with the standard coefficient. Both turbulence models are widely used in the marine and hydrodynamics application and these models have a good performance for high accuracy boundary layer simulations.

The water condition was modeled as in the experimental test, which means fresh water at 21.5 Celsius degree, (Density = 999kg/m^3, Dynamic Viscous = 1.137E-3kg/m/s). The air was assumed compressible (for computational stability reason) and was modeled with a molecular mass of 28.96kg/kmole and a Dynamic Viscosity of 1.8E-5 kg/m/s. Buoyancy forces due to fluid density difference were modeled in the analysis.

The boundary condition was employed to simulate the condition on the towing tank. A velocity inlet boundary condition was used upstream; the flow velocity was considered equal to the velocity experimental of the model using the cases of experimental measurement to wave profile. The free surface elevation was fixed at the inlet. A hydrostatic pressure outlet boundary condition was used downstream; the hydrostatic pressure at the outlet was calculated assuming an undisturbed free surface. Smooth walls with a free-slip condition were assumed for the top, floor and the side wall, only half of the model was considered in the simulations by using a symmetry plane condition at Y = 0. Smooth walls with a non-slip condition (u, v, w = 0) were assumed in the entire hull.

Convergence was assessed by plotting the flowing parameters against the number of iteration: Residuals for mass, momentum and turbulence (target criteria = 1E-4) and Drag forces (X directions). The maximum number of iterations was equal to 500. However, if the convergence criteria are reached for all residuals, the simulation was stopped before reaching 500 iterations. For most simulations, convergence of all residuals forces and monitoring points was achieved in around 300 iterations [9].

7 NUMERIC RESISTANCE VALIDATION OF THE BARE HULL

The total resistance coefficients were obtained from the numerical results and compared with the experimental value. No blockage correction was made for experimental data [4]. The speed relative to water is used in the calculation.

The total resistance coefficient is:

$$C_t = \frac{R_t}{0.5\rho . \ ^2S} \tag{17}$$

where R_t is the total resistance. The total resistance coefficient for different mesh and turbulent model are show in Figures 5 and 6.

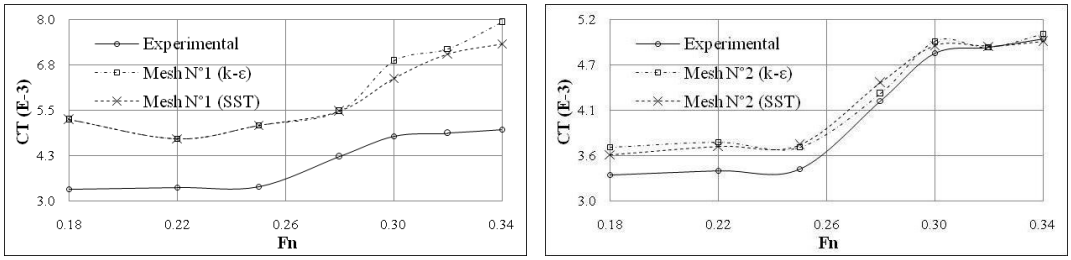

Figure 5: Total coefficient at mesh N°1 and N°2 for k-ω and k-ε turbulent model, for different Fn.

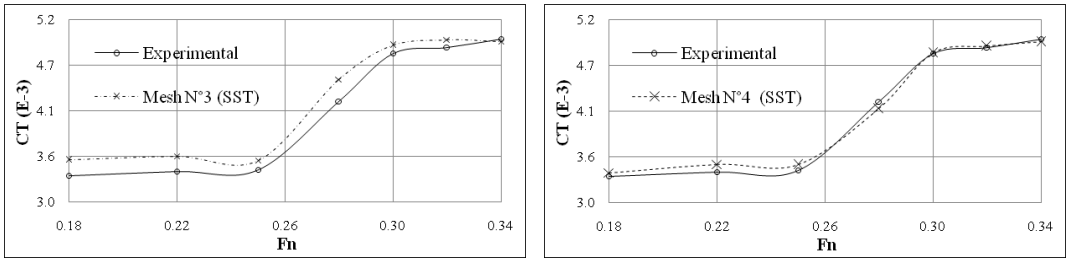

Figure 6: Total coefficient at mesh N°3 and N°4 for SST turbulent models for different Fn.

To validate the result the percentages of difference between the numerical and experimental data, were calculated and are summarized in Table 4.

Fn / Mesh N°	0.18	0.22	0.25	0.28	0.3	0.32	0.34
Mesh N°1 (SST)	80.27	67.77	84.68	102.06	138.55	166.20	179.45
Mesh N°1 (k-e)	80.03	67.77	84.68	102.06	156.04	-47.85	-59.45
Mesh N°2 (SST)	7.47	8.74	8.56	5.20	2.00	0.25	0.66
Mesh N°2 (k-e)	10.07	10.13	7.72	1.96	3.10	0.08	1.31
Mesh N°3 (SST)	7.29	5.3	3.22	6.20	2.09	1.88	0.66
Mesh N°4 (SST)	1.30	2.76	2.01	-2.09	0.16	0.29	-0.66

Table 4: Difference in percentage between C_{num} and C_{exp}

The wave pattern generated for the ship when advancing in calm water, which generate the waves on the disturbed air-water interface (free surface), is due to the ship that has to supply the energy continuously to generate the wave pattern that following the ship. Thus, the ship should overcome the drag induced by the wave generation on the free surface. The so-called wave resistance (drag) relates to this important phenomenon.

The comparison between the numerical and experimental result of the wave profile along of the hull with different Froude number and mesh size are shown in Figures 7 to 9 and the global view o the wave pattern are show in the Figure 10 and 11, at *Fn* = 0.32 for the different mesh size.

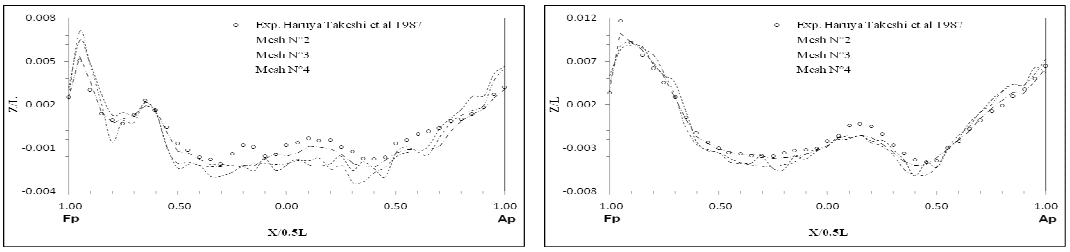

Figure 7: Predicted wave profile for *Fn* = 0.18-0.25 by CFX.

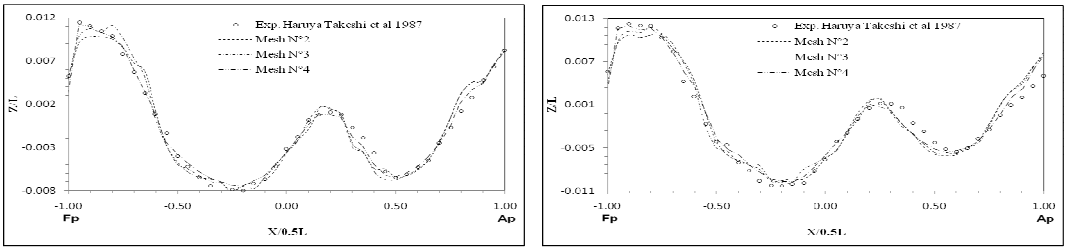

Figure 8: Predicted wave profile for *Fn* = 0.28-0.30 by CFX.

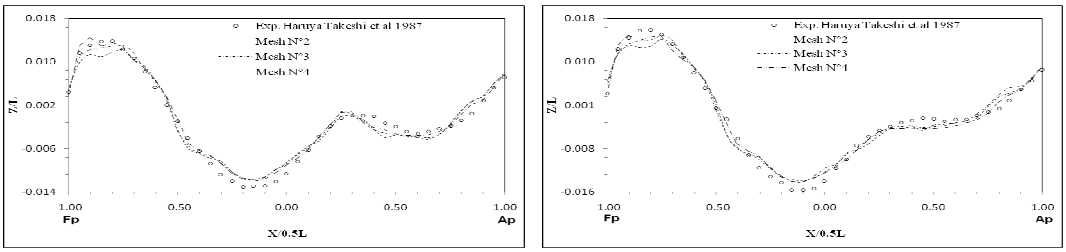

Figure 9: Predicted wave profile at *Fn* = 0.32-0.34 by CFX.

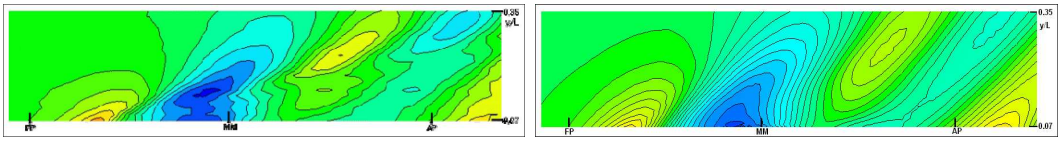

Figure 10: Experimental and predicted wave contour for mesh N°2, at *Fn* = 0.32.

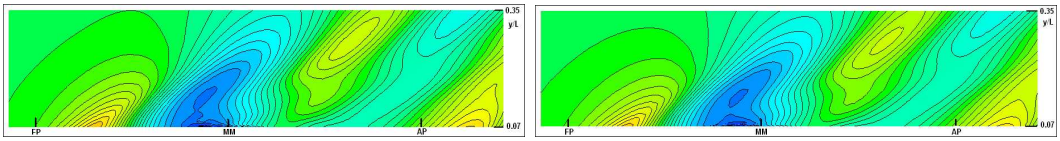

Figure 11: Predicted wave contour for mesh N°3 and N°4, at *Fn* = 0.32.

From the obtained results, it was observed that the use of prismatic mesh improves the prediction of the turbulent boundary layer, where the SST model was the best approximation. In higher Froude Number, the predicted resistance is more exact, defining a velocity range where the CFD code gives accurate results without requiring a great computational cost. For the lower Froude Number, it is necessary to use a fine mesh capable to consider small differences in the gradient of pressure and free surface deformation. The fine mesh in the interface of the fluid permits a good approximation of the wave pattern by the ship. However the fine mesh in the hull improves the prediction of the resistance better than the fine mesh in the free surface.

8 DEFINITION AND PERFORMACE OF THE IMPROVED CASES

The main objective is to minimize is the total resistance of the Series 60 model ship, in calm water at different speed for ranges of Froude number between 0.18 and 0.34. The bow of the ship was modified including two bulbs with different length. The first layout of the bulb was considered as cylinder, in which the transversal area of the cylinder was estimated as 20% of the mid ship section area and the length was considered between $0.04L_{bp}<x<0.06L_{bp}$, from the fore perpendicular. Later the shape of the bulb was modified until the proper design was achieved. The two designed bulbs are shown in Figure 11 and are compared with the naked hull.

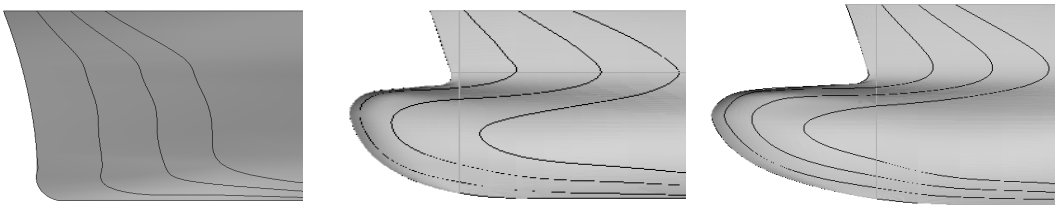

Figure 11: Perspective view of the bow and bulb geometry, naked hull, hull N°1, hull N°2

The used mesh for the hull was mesh N°2, which was used in the numerical simulation of the naked hull. For the bulb a fine mesh according to mesh N°4 was used, as show in Figure 12. The boundary condition was the same as in the previous case.

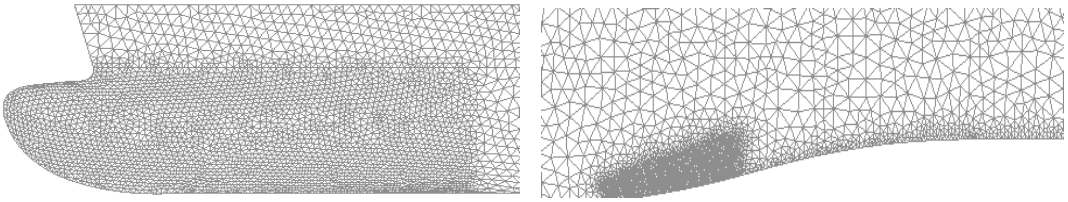

Figure 12: Mesh on the hall and free surface for the optimized cases.

The bulb reduces wave generation around the bow region. The wave generated by the bow bulb under free surface interacts with the wave generated by the design waterline. The wave resistance can be reduced if the bow bulb is properly located. The analysis of the hull with bulb, was compared with the naked hull simulation, the parameters considered in the analysis were the total resistance coefficient, the wave pattern, the wave profile along the hull, pressure in the hull and stream line in the hull, that were reported in the Figures 13 to 18 and Table 5.

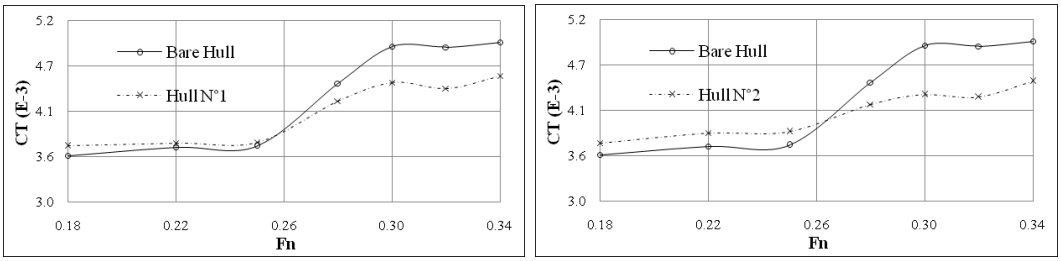

Figure 13: Total coefficient for bare hull and Hull N°1 and Hull N°2.

Fn / Hull N°	0.18	0.22	0.25	0.28	0.3	0.32	0.34
Hull N°1	-3.19	-1.46	-1.19	4.80	8.99	10.37	8.25
Hull N°2	-10.35	-10.41	-11.13	-0.99	10.61	12.73	9.73

Table 5: Difference percentage of total coefficient between bare hull and hull N°1 and hull N°2

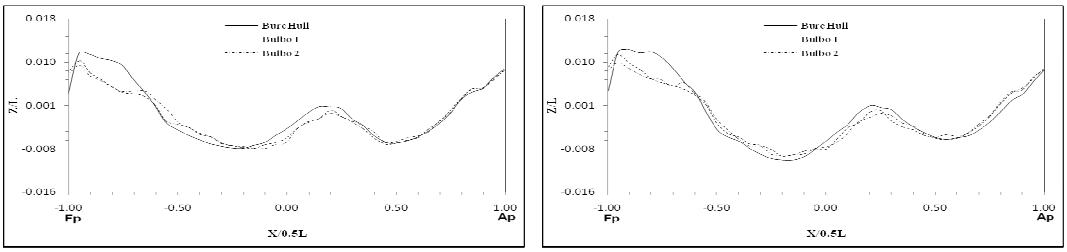

Figure 14: Predicted wave profile for hull N°1 and N°, at *Fn* = 0.28-0.30 by CFX.

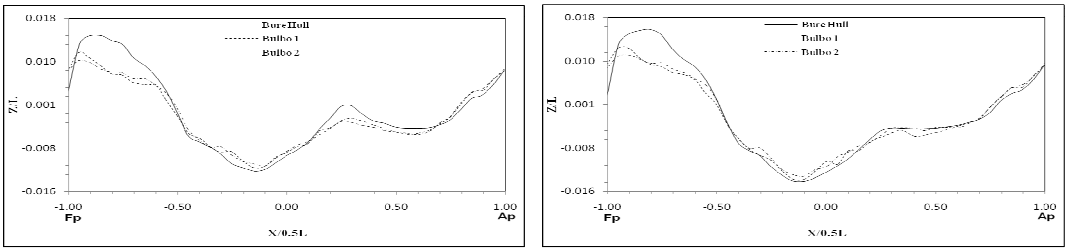

Figure 15: Predicted wave profile for hull N°1 and N°, *Fn* = 32-0.34 by CFX.

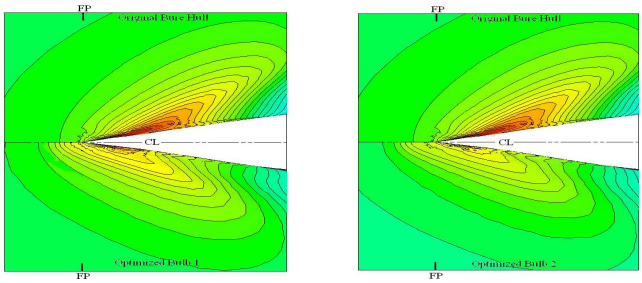

Figure 16: Predicted wave contour for hull N°1 and N°2, at *Fn* = 0.32.

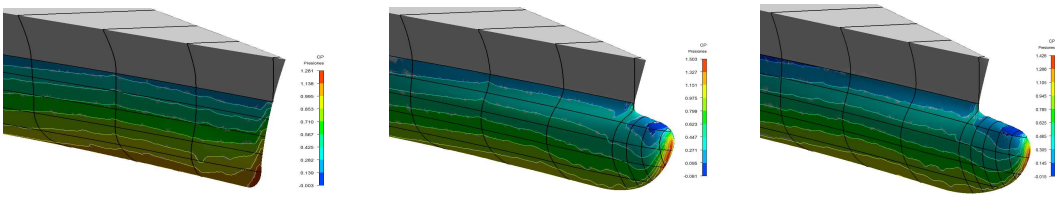

Figure 17: Pressure in the bare hull, hull N°1 and N°2, at *Fn* = 0.32.

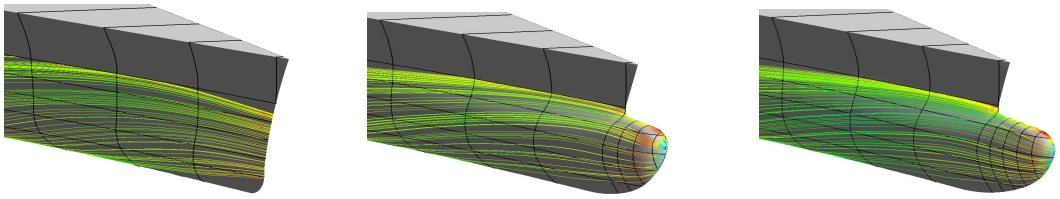

Figure 18: Steam Lines in the bare hull, hull N°1 and N°2, at *Fn* = 0.32.

The resistance in both improved hulls was reduced when a Froude number over 0.28 is used. This is observed on the computed wave pattern, as the distribution of wave field by the cussed bow bulb is globally soft and it has a smaller bow wave. The low amplitude of waves is an indication that the wave resistance component of the ship is resistance was reduced. Both improved models reduced the amplitude of the bow wave, although this is more noticeable in hull N°2. In addition, the steepness of the first wave and the first trough around both models are softer. With the bulb volume at low pressure field shows improvements in the pressure coefficient distribution. The pressure pattern on the bow varies more gently and the pressure gradients are reduced in the modified region. In the two new cases the slope of the stream lines are larger. Finally a lowest resistance was calculated from the stream flow bulb when increasing the length but this difference is marginal between both bulbs. The significant difference with the initial design is caused only by the pressure resistance, because the three cases have the same frictional resistance.

9 CONCLUSIONS

This work shows the potential of Computational Fluid Dynamics applications in ship hydrodynamic design. CFD is an effective tool allowing the optimization of the hull, which decreases the cost in the first stages of design. The viscous flow with free surface around Series 60 Model Ship was simulated for two different turbulent models at different Froude number. A comparison of these results with experimental data showed good agreement. The accuracy of the naked resistance predictions is increased when is using a mesh finer than a 0.5%*L* in the hull. The obtained results are within 10% of the experimental results. Two different bulbs were tested in CFD and provided an improvement in the hull resistance at high Froude numbers.

REFERENCES

[1] Emilio F. Campana, Daniele Peri, Yusuke Tahara and Frederick Stern, Shape optimization in ship hydrodynamics using computational fluid dynamics, *Journal Comput. Methods Appl. Mech. Engr.*196, 634–651 (2006)

[2] W. J. Kim, S. H. Van and D. H. Kim, Measurement of flows around modern commercial ship models, *Experiments in Fluid*s. 31 567-578 (2001)

[3] Suzuki H, Suzuki T, Miyazakis S, Turbulence measurement in stern flow field of a ship model – serie 60, C_B = 0.60, *Kansai Soc Nav Archit*, 227.29-40 (1997)

[4] H. Takeshi, T. Hino, M. Hinatsu, Y. Tsukada and J. Fujisawa, Flow Measurements and resistance Tests, ITTC Cooperative Experiments on a Series 60 Model At ship Research Institute, *Proc. 17th Towing Tank Conference, (ITTC)*, (1987)

[5] Bertram V, Chap K-Y, Lammers G, Laundan j, Experimental validation data free-surface flow for cargo vessel. *In: Kodoma Y (ed) Proccedings of CFD Workshop,* Tokyo Japan, 311-320 (1994).

[6] Zhang Zhi-rong, Liu Hui, Zhu Song-ping and Zhao Feng, Application of CFD In ship engineering design practice and ship hydrodynamics, *China Ship Scientific Research Center*, Wuxi 214082, China (1996)

[7] Wilcox D C, Turbulence Modelling for CFD, *DCW Industries Inc*., California, (1993)

[8] Hirt, C. W and Nichols B.D., Volume of Fluid (VOF) method for the dynamics of free boundaries, *Journal of Computational Physics*,39, 201-225 (1981)

[9] C. Craddock, A. Lebas, and A. Ganguly, Use of CFD For hull form and appendage design assessment on an offshore vessel and the identification of a wake focusing effect, *Proceedings RINA Marine CFD Symposium*, Southampton, UK, (2008)